JOURNAL OF SOLID STATE CHEMISTRY **128,** 97–101 (1997)
ARTICLE NO. SC967173

Microstructural Study of the Li^+ Ion Substituted Perovskites $Li_{0.5-3x}Nd_{0.5+x}TiO_3$

S. García-Martín,* F. García-Alvarado,† A. D. Robertson,‡ A. R. West,‡ and M. A. Alario-Franco*

* *Departamento de Química Inorgánica, Facultad de Ciencias Químicas, Universidad Complutense de Madrid, Madrid 28040, Spain;*
† *Departamento de Química Inorgánica y Materiales, Facultad de Ciencias Experimentales y Técnicas, Universidad San Pablo—CEU, Urb. Montepríncipe, 28668 Boadilla del Monte, Madrid, Spain; and* ‡ *Department of Chemistry, University of Aberdeen, Meston Walk, Old Aberdeen, AB9 2UE, Scotland, United Kingdom*

Received August 12, 1996; accepted September 25, 1996

The microstructure of samples of different polymorphs belonging to the cation-deficient $Li_{0.5-3x}Nd_{0.5+x}TiO_3$ $0.016 < x < 0.12$ solid solution has been studied by ED and TEM. The basic cell of all of them is a diagonal perovskite with dimensions $\sim\sqrt{2}a_p \sim \sqrt{2}a_p \sim 2a_p$. However, important differences between the polymorphs have been found in the microstructure. While in *C*-phase samples a randomly oriented microdomain structure of the basic cell is found, for the β polymorph materials a more complex domain microstructure gives rise to a very large superperiodicity ($a = 58.6$ Å $b = 90.7$ Å) as is also the case for the α' polymorph samples.

I. INTRODUCTION

There has been great interest in the study of Li^+ ion conductors of general formula $Li_{0.5-3x}RE_{0.5+x}TiO_3$ since Inaguma *et al.* reported in 1993 a very high value of lithium conductivity in $La_{0.51}Li_{0.34}TiO_{2.94}$ ($\sigma = 1 \times 10^{-3}$ S cm^{-1} at 25°C) (1–4).

It is well known that these kinds of materials are perovskite-related but there is some uncertainty as to their structural crystal chemistry due to the disagreement of the published results (5–8).

Recently, Robertson *et al.* reported a phase diagram study of the $Li_{0.5-3x}RE_{0.5+x}TiO_3$ (RE = La, Nd) systems showing the stoichiometry ranges, thermal stabilities, and polymorphism of both perovskite-related solid solutions (9). The existence range for the $Li_{0.5-3x}La_{0.5+x}TiO_3$ solid solution was $0.025 < x < 0.13$, and $0.016 < x < 0.12$ for the Nd system. Depending on the temperature and composition, three different polymorphs labeled α, β, and A were found in the La system and four, α', β, A, and C, in the Nd system. Besides, it seems that the phase transitions between the polymorphs were largely continuous in character in both systems.

The crystal structure of one member of the C polymorph of the solid solutions $Li_{0.5-3x}Nd_{0.5+x}TiO_3$ ($x = 0.05$), determined from powder neutron diffraction, shows that it is a $GdFeO_3$-type perovskite, partially collapsed in all three directions by means of a cooperative tilting and rotating of the octahedra (10). This collapsing of the structure is likely due to the combined effect of the size of Nd cations, the Li^+ ions in off-center sites, and the occurrence of A-site vacancies. Although, in this case, short-range order was not found, a microstructural study of these solid solutions appears to be necessary due to the complexity of the A cation sublattice which could adopt different ordering states and produce different structural distortions.

We present here a microstructural study of the C, α', and β polymorphs of the $Li_{0.5-3x}Nd_{0.5+x}TiO_3$ solid solution, studied by electron diffraction and high resolution electron microscopy.

II. EXPERIMENTAL

Samples were prepared as described in Ref. (9) from appropriate amounts of Li_2CO_3, Nd_2O_3, and TiO_2. The mixtures were pelleted, covered with powder of the same composition to prevent lithia loss and fired at 1100°C for one day followed by further grinding, repelleting, and refiring at 1200°C for another day. For phase diagram studies, small samples were annealed isothermally and quenched to room temperature.

For crystalline phase identification a Philips–Hagg–Guinier camera was used. The determination of the lattice parameters were achieved using a STOE STADI P diffractometer in transmission mode with a small linear position sensitive detector, Ge monochromator and Cu$K\alpha_1$ radiation.

For transmission electron microscopy, the samples were crushed in an agate mortar and ground in *n*-butyl alcohol. A few drops of the resulting suspension were deposited on

0022-4596/97 $25.00

a carbon-coated copper grid. Electron diffraction studies were performed in an electron microscope JEOL 2000FX (double tilt $\pm 45^{\circ}$) while for high resolution electron microscopy, an electron microscope JEOL 4000EX (double tilt $\pm 25^{\circ}$) was used.

III. RESULTS AND DISCUSSION

C Polymorph

The unit cell of *C*-phase samples was indexed from X-ray powder diffraction as an orthorhombic cell with lattice parameters related to the basic perovskite subcell as follows: $a \sim \sqrt{2}a_p$, $b \sim \sqrt{2}a_p$, $c \sim 2a_p$. The structure was determined from neutron powder diffraction analysis using the same cell but with the *b* and *c* axes interchanged, i.e., $a \sim \sqrt{2}a_p$, $b \sim \sqrt{2}a_p$, $c \sim 2a_p$, and S.G. *Pnma* (10).

Figure 1 shows two electron diffraction patterns of *C*-$Li_{0.5-3x}Nd_{0.5+x}TiO_3$ ($x = 0.05$) corresponding to two different zones of the reciprocal lattice. The patterns were indexed using a $\sim \sqrt{2}a_p \sim 2a_p \sim \sqrt{2}a_p$ cell and no superlattice reflections of this cell were observed. However, the patterns show some reflections ($(0\,k\,0)$ $k = 2n + 1$, $(h\,0\,0)$ $h = 2n + 1$) that do not fit the *Pnma* space group. These reflections might be consistent with the *Pmmm* space group. A remnant of the (0 1 0) reflection, which is forbidden in the *Pnma* S.G., was observed in the neutron diffraction profile but the reflection was very broad. This may indicate the presence of small domains with a local structure consistent with the *Pmmm* S.G. within an overall *Pnma* long-range order. Apart from this, weak diffuse streaks parallel to $g_{100d} \| g_{101p}$ can be seen in Fig. 1a (subindex d refers to the diagonal cell while subindex p refers to the basic cubic perovskite cell).

Figure 2a shows an electron diffraction pattern corresponding to *C*-$Li_{0.5-3x}Nd_{0.5+x}TiO_3$ with $x = 0.025$. The pattern can be indexed using either a $\sim 2a_p$, $\sim 2a_p$, $\sim 2a_p$ cell or domains of a $\sim \sqrt{2}a_p$, $\sim 2a_p$, $\sim \sqrt{2}a_p$ in circular permutation which would be in agreement with the previous patterns. The micrograph shown in Fig. 2b corresponds to an image of a microcrystal oriented in the same zone axis as the microcrystal shown in Fig. 2a. It shows a patchwork-quilt array where there are two regions in which 7.6 Å fringes are parallel to g_{100p} and other regions in which the 7.6 Å fringes are parallel to g_{010p}. The crystal is then formed by microdomains of $\sim \sqrt{2}a_p$, $\sim 2a_p$, $\sim \sqrt{2}a_p$ unit cell, where in each domain the *b*-axis is oriented along one of the three different crystallographic directions (11, 12). The microdomains appear randomly distributed so that the electron diffraction pattern obtained in Fig. 2a is composed just by the overlapping of three electron diffraction patterns, each one produced by the respective microdomain. This type of microdomain structure was also observed on some crystals with $x = 0.05$.

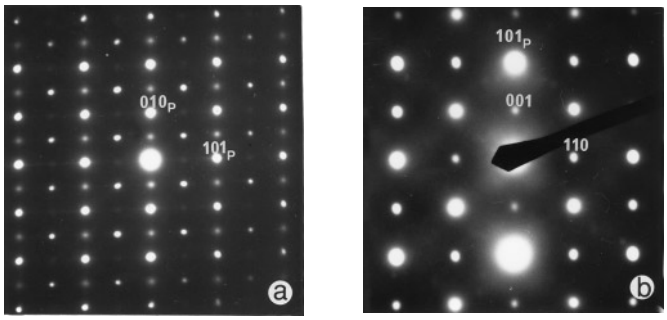

FIG. 1. Electron diffraction patterns of *C*-$Li_{0.5-3x}Nd_{0.5+x}TiO_3$, $x = 0.05$ (a) $[0\,0\,1] = [1\,0\,\bar{1}]_p$ zone diffraction pattern and (b) $[\bar{1}\,1\,0]$ zone diffraction pattern.

Therefore, the structure of the *C*-phase appears to be based in a three-dimensional framework of corner-sharing TiO_6 octahedra in the three directions leading to an orthorhombic perovskite-related cell of lattice parameters $\sim \sqrt{2}a_p$, $\sim 2a_p$, $\sim \sqrt{2}a_p$. Moreover, most of the crystals of this phase are formed by randomly distributed microdomains related to each other by 90° rotations. The existence of diffuse bands parallel to g_{100d} suggest some kind of planar disorder. No differences on the electron diffraction patterns were found in samples with different composition.

β Polymorph

The lower temperature *β*-polymorph sample also has a perovskite-related structure and the lattice parameters deduced from powder X-ray diffraction data were $a = b \sim a_p$, $c \sim 2a_p$ (9).

Figure 3 shows differently oriented electron diffraction patterns corresponding to a sample with $x = 0.1$. The features of the patterns point to a rather more complicated microstructure than that observed for the *C*-phase compounds.

The pattern shown in Fig. 3a exhibits, besides the basic perovskite cell, two different sets of spots. The first one appears around the $(h\,0\,0)_p$ and $(0\,k\,0)_p$ spots and is formed by four quite strong satellites and some more of weaker intensity. Around $(h/2\,k/2\,0)_p$ we find the second set, showing four strong spots arranged like a cross and weak satellites along the diagonals of the cross. We can consider the last set as a reflection at $(h/2\,k/2\,0)_p$ replaced by a cluster of four satellite reflections in the form of crosses whose arms are parallel to g_{100p} and g_{010p}.

Figure 3b shows a $[0\,1\,0]_p$ zone diffraction pattern. Superlattice reflections of the type $(h\,0\,1/2)_p$, doubling c_p, are observed as well as two satellite reflections around $(h\,0\,0)_p$. The $[\bar{1}\,0\,2]_p$ an $[\bar{1}\,0\,4]_p$ zone diffraction patterns, Figs. 3c and 3d, respectively, also show a doubling of c_p and a satellite arrangement similar to the one observed in Fig. 3a.

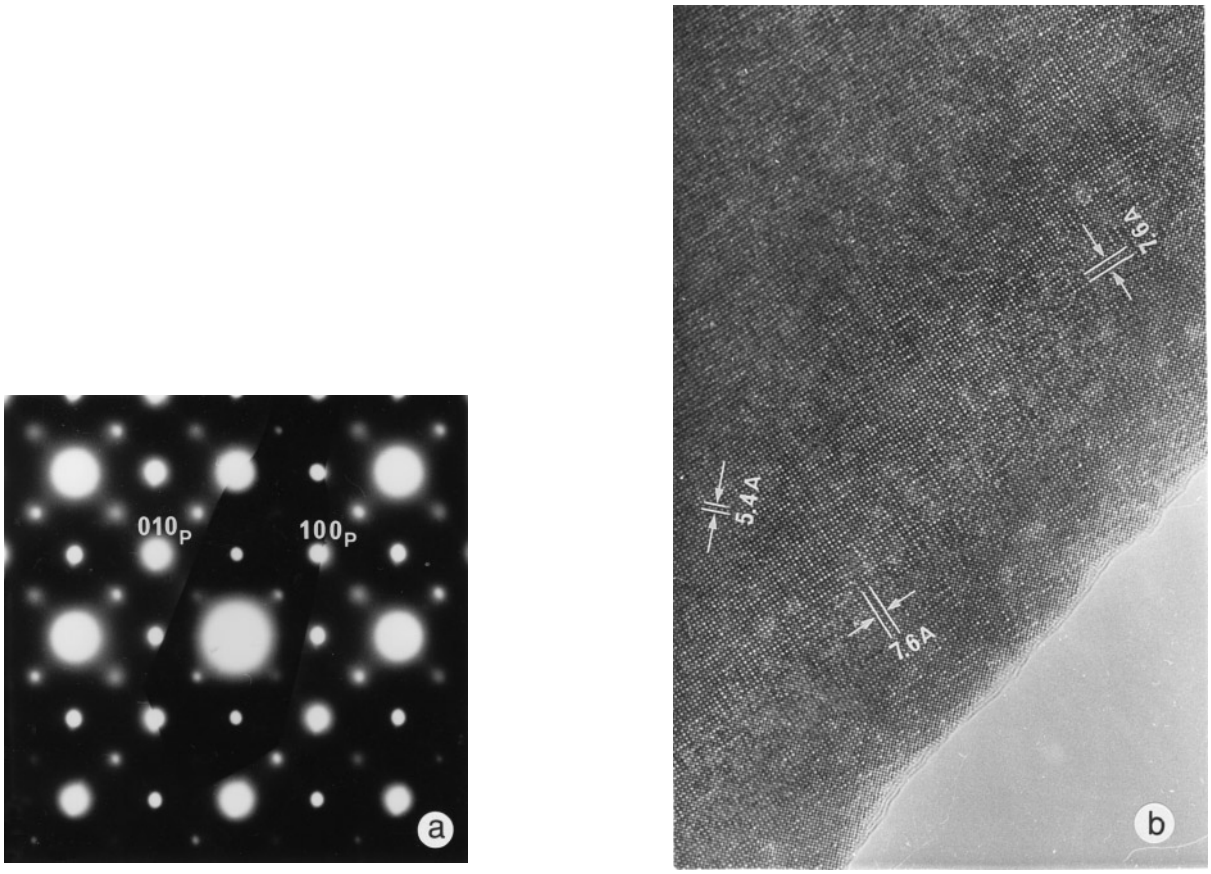

FIG. 2. Electron diffraction/microscopy of C-$Li_{0.5-3x}Nd_{0.5+x}TiO_3$, $x = 0.025$ (a) $[0\,0\,1]_p$ zone diffraction pattern and (b) image corresponding to the $[0\,0\,1]_p$ diffraction pattern in (a).

Figure 3e shows a $[1\,1\,0]_p$ zone diffraction pattern: the extra weak reflections at $(h/2\,h/2\,l)_p$ are the intersection of the "crosses" observed in Fig. 3a with the $[1\,1\,0]$ zone due to the slight curvature of the Ewald sphere.

The combination of all these observations suggest the reciprocal lattice shown in Fig. 4.

Taking into account only the main reflections of these patterns, i.e., without the satellites, it appears that the basic unit cell of this phase is $\sim\sqrt{2}a_p$, $\sim\sqrt{2}a_p$, $\sim 2a_p$, different than the one deduced from the X-ray powder diffraction results ($a = b = a_p$ $c \sim 2a_p$) but similar to the one shown above for the C-phase. By analogy with other perovskite materials (16) and the C-phase samples of the $Li_{0.5-3x}Nd_{0.5+x}TiO_3$ solid solution, we ascribe the reflection at $(h/2\,k/2\,l)_p$ to tilting of the oxygen octahedral framework. As in $GdFeO_3$ (13) or $CaTiO_3$, the presence of the $(h/2\,k/2\,l)$ reflection that gives place to the diagonal cell can be related to a coordinated tilting of the octahedral framework which is described either as a correlated tilting around the three unit cell axes (14) or as tilting around a diagonal direction (15). However, in this case, these reflections are split into four satellites forming a cross with arms parallel to g_{100p} and g_{010p}. The separation between pairs of split spots indicates superperiods of $\sim 7a_p$ (28 Å) and $\sim 11b_p$ (43.3 Å), respectively, along g_{100p} and g_{010p}. This splitting might be due to a quasiperiodic microdomain structure in which the system of octahedral tilts is twinned across intersecting $(1\,0\,0)_p$ and $(0\,1\,0)_p$ domain boundaries with average separations of $\sim 3.5a_p$ and $\sim 5.5b_p$ as has been observed in other A cation deficient perovskite materials (16–18).

The four strong satellites in an approximately rectangular configuration around $(h\,0\,0)_p$ and $(0\,k\,0)_p$ in Fig. 3a suggest a two-dimensional noncommensurate modulation with superperiods of ~ 44.8 Å along g_{320p} and $g_{\bar{3}20p}$. This modulation is also observed around the four spots forming a cross at $(1/2\,1/2\,l)_p$. Again by analogy with the A cation deficient perovskites, this superperiodicity is most likely due to an ordering between Li, Nd, and vacancies within the A sublattice probably coupled to the microdomains formed by the system of the tilted octahedra.

Figure 3f shows an image corresponding to the diffraction pattern in Fig. 3a. It shows a patchwork-quilt array characteristic of the existence of microdomains in which 7.6 Å

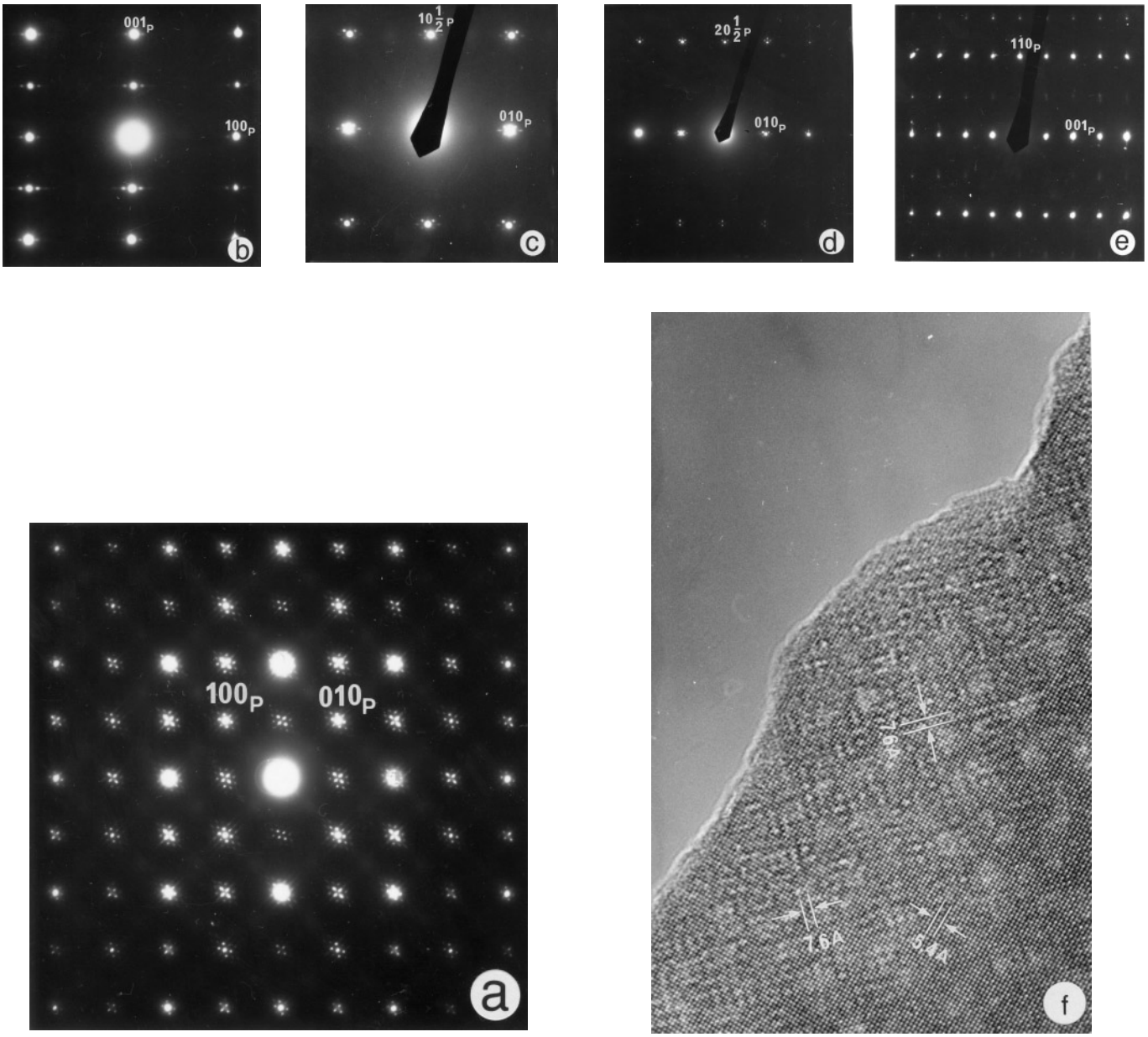

FIG. 3. Electron diffraction/microscopy of β-$Li_{0.5-3x}Nd_{0.5+x}TiO_3$, $x = 0.1$ (a) $[0\,0\,1]_p$ zone diffraction pattern, (b) $[0\,1\,0]_p$ zone diffraction pattern, (c) $[\bar{1}\,0\,2]_p$ zone diffraction pattern, (d) $[\bar{1}\,0\,4]_p$ zone diffraction pattern, (e) $[1\,\bar{1}\,0]_p$ zone diffraction pattern, and (f) image corresponding to the $[0\,0\,1]_p$ diffraction pattern in (a).

fringes are either parallel to g_{100p} or to g_{010p}. As was observed for the *C*-phase samples, the crystal is formed by microdomains of $\sim\sqrt{2}a_p$, $\sim\sqrt{2}a_p$, $\sim 2a_p$ unit cell, where in each domain, the *c*-axis is oriented along one of the three different crystallographic directions. These microdomains are randomly distributed and their size is very small. This is probably the reason why the intensity of the spots at $(h/2\,0\,0)_p$ and $(0\,k/2\,0)_p$ is so weak. Larger periodicities are not distinguished in this micrograph.

Other members of the solid solution with β-phase structure and various compositions corresponding to $x = 0.025$, 0.075, and 0.112 were investigated. However no significant microstructural differences were found.

α′-Polymorph

Again, the microstructural study performed on samples belonging to this phase showed no significant differences

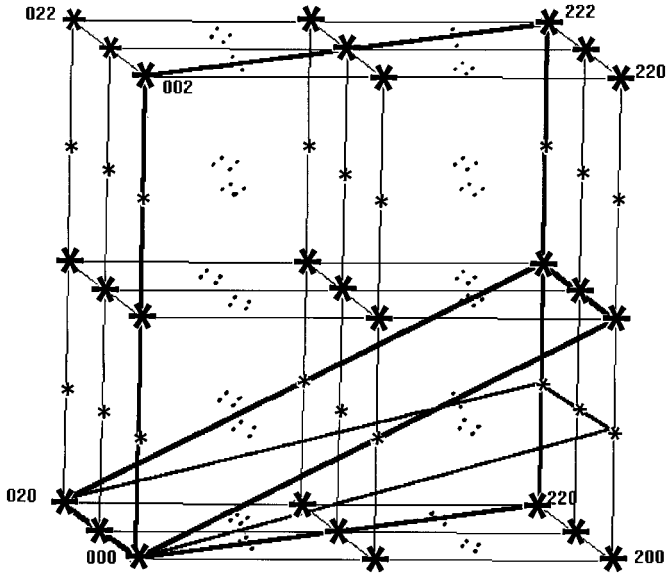

FIG. 4. Drawing of the reciprocal lattice of β-$Li_{0.5-3x}Nd_{0.5+x}TiO_3$ showing the diffraction effects as they are observed to occur in the electron diffraction patterns in Fig. 3.

with respect to the β-polymorph ones. This led us to believe that both β and α' are the same phase.

CONCLUSIONS

The electron diffraction and high resolution electron microscopy study of the $Li_{0.5-3x}Nd_{0.5+x}TiO_3$ solid solution shows that three (C, α', and β) of the four different polymorphs established in the phase diagram study of these compounds (9) have a common basic unit cell with lattice parameters $\sim\sqrt{2}a_p$, $\sim\sqrt{2}a_p$, $\sim 2a_p$. The distortion of the perovskite structure in these materials is most likely due to the tilting of the octahedra framework along the three crystallographic directions as it has been determined for the C-phase samples by neutron diffraction analysis (10).

Another general feature of the three polymorphs of these compounds is the existence of a domain structure, where each domain has a different orientation of the $c = 2a_p$-axis along one of the three crystallographic directions.

Apart from this, the β-phase samples show another, more complicated ordering which is not observed in the C-phase compounds. A system of octahedral tilts is twinned across intersecting $(1\,0\,0)_p$ and $(0\,1\,0)_p$ domain boundaries forming a microdomain structure. The presence of a very large superperiodicty (~ 44.8 Å along g_{320p} and $g_{\bar{3}20p}$) indicates a possible additional long-range ordering of Li, Nd, and vacancies within the microdomains.

Moreover, the complex different microstructures found for the C, α', and β polymorphs show no variation with composition within their corresponding existence ranges. In any case, the explanation of such differences would require the solution of the crystal structures.

REFERENCES

1. Y. Inaguma, C. Liquan, M. Itoh, T. Nakamura, T. Uchida, H. Ikuto, and M. Wakihara, *Solid State Commun.* **86,** 689 (1993).
2. Y. Inaguma, L. Chen, M. Itoh, and T. Nakamura, *Solid State Ionics* **70/71,** 196 (1994).
3. M. Itoh, Y. Inaguma, W. H. Jung, L. Chen, and T Nakamura, *Solid State Ionics* **70/71,** 203 (1994).
4. H. Kawai and J. Kuwano, *J. Electrochem. Soc.* **141,** 278 (1994).
5. J. Brous, I. Fankuchan, and E. Bans, *Acta Crystallogr.* **6,** 67 (1953).
6. P. V. Patil and V. S. Chincholkar, *Indian J. Chem. A* **16,** 161 (1978).
7. A. M. Varaprasad, A. L. Shashi Mohan, D. K. Chakrabarty, and A. B. Biswas, *J. Phys. C* **12,** 465 (1979).
8. I. L. Kochergina, N. B. Khakhin, N. V. Porotnikov, and K. I. Petrov, *Russian J. Inorg. Chem.* **29,** 506 (1984).
9. A. D. Robertson, S. García-Martín, A. Coats, and A. R. West, *J. Mater. Chem.* **5**(9), 1405 (1995).
10. J. M. S. Skakle, G. C. Mather, M. Morales, R. I. Smith, and A. R. West, *J. Mater. Chem.* **5**(11), 1807 (1995).
11. T. J. White, R. L. Segall, J. C. Barry, and J. L. Hutchison, *Acta Cryst. B* **41,** 93 (1985).
12. M. Vallet-Regi, J. M. González-Calbet, J. Verde, and M. A. Alario-Franco, *J. Solid State Chem.* **57,** 197 (1985).
13. M. Marezio, J. P. Remeike, and P. D. Dernier, *Acta Cryst. B* **26,** 2008 (1970).
14. A. M. Glazer, *Acta Cryst. B* **28,** 3384 (1972).
15. M. O'Keeffe and B. G. Hyde, *Acta Cryst. B* **33,** 3802 (1977).
16. M. Labeau, thesis, I.N.P. Grenoble, 1980.
17. M. A. Alario-Franco, I. E. Grey, J. C. Joubert, H. Vincent, and M. Labeau, *Acta Cryst A* **38,** 177 (1982).
18. M. Labeau, I. E. Grey, J. C. Joubert, H. Vincent, and M. A. Alario-Franco, *Acta Cryst A* **38,** 753 (1982).